Redox Biology 41 (2021) 101931

Contents lists available at ScienceDirect

Redox Biology

journal homepage: www.elsevier.com/locate/redox

Short Communication

Regulation of dual oxidase hydrogen peroxide synthesis results in an epithelial respiratory burst

Gregory E. Conner

Department of Cell Biology, University of Miami Miller School of Medicine, 1600 NW 10th Avenue, Miami, Fl, 33136, USA

ARTICLE INFO

Keywords:
NADPH oxidase
Duox
Hydrogen peroxide
Cell redox status

ABSTRACT

Redox status is a central determinant of cellular activities and redox imbalance is correlated with numerous diseases. NADPH oxidase activity results in formation of H_2O_2, that, in turn, sets cellular redox status, a key regulator of cellular homeostasis and responses to external stimuli. Hydrogen peroxide metabolism regulates cell redox status by driving changes in protein cysteine oxidation often via cycling of thioredoxin/peroxiredoxin and glutathione; however, regulation of enzymes controlling synthesis and utilization of H_2O_2 is not understood beyond broad outlines. The data presented here show that calcium-stimulated epithelial Duox H_2O_2 synthesis is transient, independent of intracellular calcium renormalization, H_2O_2 scavenging by antioxidant enzymes, or substrate depletion. The data support existence of a separate mechanism that restricts epithelial H_2O_2 synthesis to a burst and prevents harmful changes in redox tone following continuous stimulation. Elucidation of this H_2O_2 synthesis tempering mechanism is key to understanding cellular redox regulation and control of downstream effectors, and this observation provides a starting point for investigation of the mechanism that controls H_2O_2-mediated increases in redox tone.

1. Introduction

H_2O_2 plays important roles in host defense, hormone synthesis, fertilization, embryogenesis and development, signal transduction, animal and plant cell differentiation and growth, cell death et al. [1,2]. For example, H_2O_2 levels control specific transcriptional regulation via OxyR in *E. coli* [3], activation of ion channels to regulate root growth in plants [4,5], and modulation of tyrosine phosphorylation via phosphatase oxidation in mammalian cells [6], all of which rely on thiol-disulfide switches to alter protein function. Both B-cell and T-cell receptor signaling are regulated by H_2O_2 [7,8]. Disrupted redox modulation of protein activities is associated with a variety of pathologies [9]. Specific enzyme systems, such as the thioredoxin and glutathione systems, have evolved to use and scavenge H_2O_2; however, H_2O_2 synthesis appears to control overall cellular redox tone. Thus, cellular redox state is primarily controlled by H_2O_2 synthesis and cellular NADPH oxidases are the major regulatable H_2O_2 source in eukaryotic cells.

2. Methods

Cells. Normal bronchial epithelial cells were isolated from lungs of de-identified organ donors whose lungs were not used for transplant and were provided with consent by the Life Alliance Organ Recovery Association (LAORA, Department of Surgery, U. Miami). Our Institutional Review Board has determined that the consent for organ donation for research covers research uses of this material. Cells were isolated, expanded and redifferentiated in air-liquid interface culture as described previously [21,22]. Isolation and growth of HEK293T cells expressing either DUOX1/DUOXA1α or DUOX2/DUOXA2 were previously described [16].

Assays and measurements. H_2O_2 synthesis assays on intact cells in culture have been described previously [16]. For homogenization and assay, cells were washed with ice cold PBS containing 0.25 mM EDTA and twice with homogenization buffer containing 25 mM K acetate, 10 mM HEPES, pH 7.6, 1 mM MgCl2, 10 μM leupeptin, benzamidine, aprotinin, pepstatin, PMSF, 1 mM β-glycerophosphate and Na pyrophosphate and scraped into homogenization buffer. After 20 min on ice, cells were pelleted at 300×*g*, resuspended in homogenization buffer (0.7 ml/100 mm dish), and homogenized 10–15 strokes with a tight fitting Dounce homogenizer. Cell breakage was monitored with phase contrast microscopy and terminated with addition of 2.5 M sucrose to 0.25 M and mixing. Homogenates were snap frozen in liquid N_2 and stored at −80°.

Abbreviations: NHBE, normal human bronchial epithelia; HRP, horseradish peroxidase.

E-mail address: gconner@miami.edu.

https://doi.org/10.1016/j.redox.2021.101931
Received 21 January 2021; Received in revised form 19 February 2021; Accepted 1 March 2021
Available online 5 March 2021

Membrane fractions were prepared from homogenates by 1000×*g* centrifugation for 5 min at 4° and then collected from the supernatant by 20,000×*g* centrifugation for 30 min and resuspended in homogenization buffer.

H_2O_2 synthesis by HEK homogenates and membrane fractions were assayed in a BioTek Synergy H1 plate reader at 27°. This temperature was chosen as it is the lowest regulatable temperature in the plate reader operating at room temperature and reduced possible temperature related destabilization of the enzyme that might occur at higher temperatures. Reaction buffers contained 25 mM HEPES or 50 mM Na PO_4, pH 7.2, 1 μM FAD, various chelated [$CaCl_2$] (see below), 1.5 mM $MgCl_2$, 0.1 μM Thapsigargin, 30 μM Amplex red (10-Acetyl-3,7-dihydroxyphenoxazine, Cayman Chemical, Ann Arbor MI) and 0.15 U/ml HRP (cat #P2088, Sigma Aldrich, St Louis MO). Enzyme and/or homogenization buffer was added to 5% of the assay volume. After a 5 min baseline recording to allow temperature equilibration, 50 μM NADPH was added by automated injection and mixing, and fluorescence (ex535 nm, em 590 nm) was continuously recorded at 20–40 s intervals. H_2O_2 was quantified by comparison to H_2O_2 standard curves performed in buffer identical in composition to that used for each individual enzyme assay. Rates were calculated as the slope of the fluorescence change typically over 120 s using a 20–40 s sliding window. H_2O_2 values were normalized to assays containing homogenates or membrane fractions from cells transduced with empty viruses, which eliminates NADPH background signal seen in HRP/Amplex Red assays.

Post-hoc measurement of H_2O_2 synthesis was performed using reaction mixtures, described above but without Amplex red and HRP and with 1 mM NaN_3 to inhibit catalase. Reactions were stopped at time intervals by injection of H_3PO_4 to 0.1 M and NADPH fluorescence was used to confirm NADPH loss. Samples were then neutralized with Na_2HPO_4 and assayed with Amplex red and HRP. NADPH fluorescence was followed using 340 nm excitation and 460 nm emission to confirm enzyme activity in the absence of Amplex red HRP and to confirm acid decomposition after addition of H_3PO_4. NADPH concentrations were determined using molar extinction coefficient at 340 nm = 6320 M^{-1} cm^{-1}. Real-time quantification of NADPH was performed by following fluorescence (ex340, em460) and comparison to absorption standards.

Intracellular calcium levels were measured and calculated as described previously [16] using ratiometric recordings of Fura-2 fluorescence with emission at 475 nm to prevent interference by resorufin absorbance. Chelated Ca^{2+} solutions for assays were buffered with EGTA, NTA, and HEGTA, and [Ca^{2+}] calculated using WEBMAXC Extended program (https://somapp.ucdmc.ucdavis.edu/pharmacology/bers/maxchelator/webmaxc/webmaxcE.htm). Calcium concentrations were checked by ion selective electrode using manufacturer standards (Kwickcal-2 electrode, WPI Inc).

Oxygen consumption was measured using Mito-ID (Enzo 51047, ENZO Life Sciences), a fluorescent oxygen sensor probe, according to the manufacturer's specification. Probe was added to assays mixtures containing calcium and NADPH, no Amplex Red or HRP, and no enzyme for baseline recording, followed by addition of homogenates or buffer. Time resolved fluorescence was recorded using a BioTek H1 plate reader with 380 nm excitation and 650 nm emission with 30 μs integration window at 30 and 70 μs.

3. Results and discussion

DUOX1 and DUOX2 are expressed in a variety of epithelial cells and their tissue distributions have been determined previously by several groups. The importance of DUOX1 and DUOX2 is fully appreciated by comparison of their expression levels relative to other non-phagocytic NADPH oxidases. In most epithelial cells, DUOX1 and DUOX2, are expressed at higher levels than any of the other non-phagocytic NADPH oxidases and DUOX1 is the major non-phagocytic NOX form in the brain (Fig. 1A). Thus, DUOX1 and DUOX2 may be the major contributors of regulated H_2O_2 synthesis in most epithelia. These enzymes contain calcium binding EF-hand motifs for activation by intracellular calcium transients [10], and thus, purinergic receptor stimulation [11,12] or addition of ionomycin [13] lead to simultaneous rapid increases in intracellular [Ca^{2+}] ([Ca^{2+}]$_i$) and Duox activity. To assess the temporal correspondence of Duox H_2O_2 synthesis with [Ca^{2+}]$_i$ changes, fully differentiated normal human bronchial epithelia (NHBE) in air-liquid interface cultures were simultaneously assayed for H_2O_2 synthesis and [Ca^{2+}]$_i$ after either apical ATP stimulation or ionomycin (Fig. 1B-F). In addition to often-used progress curves of H_2O_2 accumulation vs. time [e.g. 14] (Fig. 1B and E), H_2O_2 synthesis data were plotted as rates (Fig. 1C, D and F) allowing comparison of activity with [Ca^{2+}]$_i$ changes. As expected, purinergic stimulation or ionomycin and thapsigargin treatment were followed by an immediate [Ca^{2+}]$_i$ increase and a coincident increase in H_2O_2 synthesis. ATP-stimulated Duox activity was transient but fell more slowly than [Ca^{2+}]$_i$. Surprisingly in the case of ionomycin, H_2O_2 synthesis still declined despite continued elevation of [Ca^{2+}]$_i$ (Fig. 1D). Therefore, Duox activity was terminated independent of decreasing [Ca^{2+}]$_i$.

Two trivial explanations for transient Duox activity were experimentally addressed. It was possible that the HRP/Amplex red H_2O_2 assay system was exhausted or that intracellular NADPH substrate pools were inadequate to maintain synthesis. To test these possibilities, NHBE cultures were sequentially stimulated, first with ATP and then again by ionomycin after the ATP-stimulated H_2O_2 synthesis and [Ca^{2+}]$_i$ declined (Fig. 1E and F). The data showed Duox activity could be re-stimulated in the same culture after a first transient response to increased [Ca^{2+}]$_i$. Thus, the assay system was not depleted and the data strongly suggested the NADPH pool was not limiting. A slight difference was noted between purinergic and ionophore stimulation, with decay of purinergic stimulated H_2O_2 synthesis slower than that following ionomycin where [Ca^{2+}]$_i$ remained elevated. This was a reproducible difference unrelated to sequential additions (viz. Fig. 1C and D vs Fig. 1F).

Others have observed transient H_2O_2 accumulation by non-phagocytic NADPH oxidases and ascribed this to consumption of H_2O_2 by anti-oxidant enzymes rather than regulation of oxidases [15]. The assay used here targets cell surface, extracellular H_2O_2 and contains high HRP levels to generate fluorescent signal, effectively competing for H_2O_2 against low levels of extracellular glutathione peroxidase or peroxiredoxin. Nevertheless, assay of intact cells might detect H_2O_2 synthesized by cytoplasmic enzyme, that diffuses out of cells and could be modulated by intracellular enzyme catabolism. To rule out consumption of Duox-synthesized H_2O_2 by intracellular anti-oxidant enzymes and to further explore possible substrate depletion, HEK293T cells, made to express DUOX1/DUOXA1α or DUOX2/DUOXA2 [16], were used to study Duox in a cell-free system.

Intact Duox-expressing HEK293T cells showed similar transient responses in constantly elevated [Ca^{2+}]$_i$ following ionomycin (Fig. 2A and B). In Duox-expressing cell-free homogenates, H_2O_2 synthesis following addition of NADPH to Ca^{2+}-containing buffers slowed with kinetics similar to intact cells (Fig. 2C–F). Thus, activity declined in constant [Ca^{2+}] *in vitro* as well as *in vivo*. The decay of Duox activity was also seen in post-mitochondrial membrane fractions (Fig. 2G). Auranofin (2 μM), that inhibits H_2O_2 utilization by glutathione and thioredoxin cycling [17], did not prevent termination of activity (Fig. 2C–F). To the contrary, auranofin inhibited DUOX1, but not DUOX2, H_2O_2 synthesis suggesting that DUOX1 redox status may play a role in regulating activity. Consumption of NADPH was measured simultaneously with Amplex red oxidation after addition of auranofin. In assays of DUOX2 homogenates, auranofin did not significantly alter NADPH consumption although it was reduced in DUOX1 homogenates coincident with reduction of H_2O_2 synthesis (Supplementary Figs. S1A–B). Thus, intracellular H_2O_2 consumption is unlikely to account for the apparent loss of Duox activity.

To assess effects of NADPH consumption on H_2O_2 synthesis, NADPH was re-added to assays after loss of activity but did not restore rates (Supplementary Fig. S1C), confirming that NADPH consumption did not

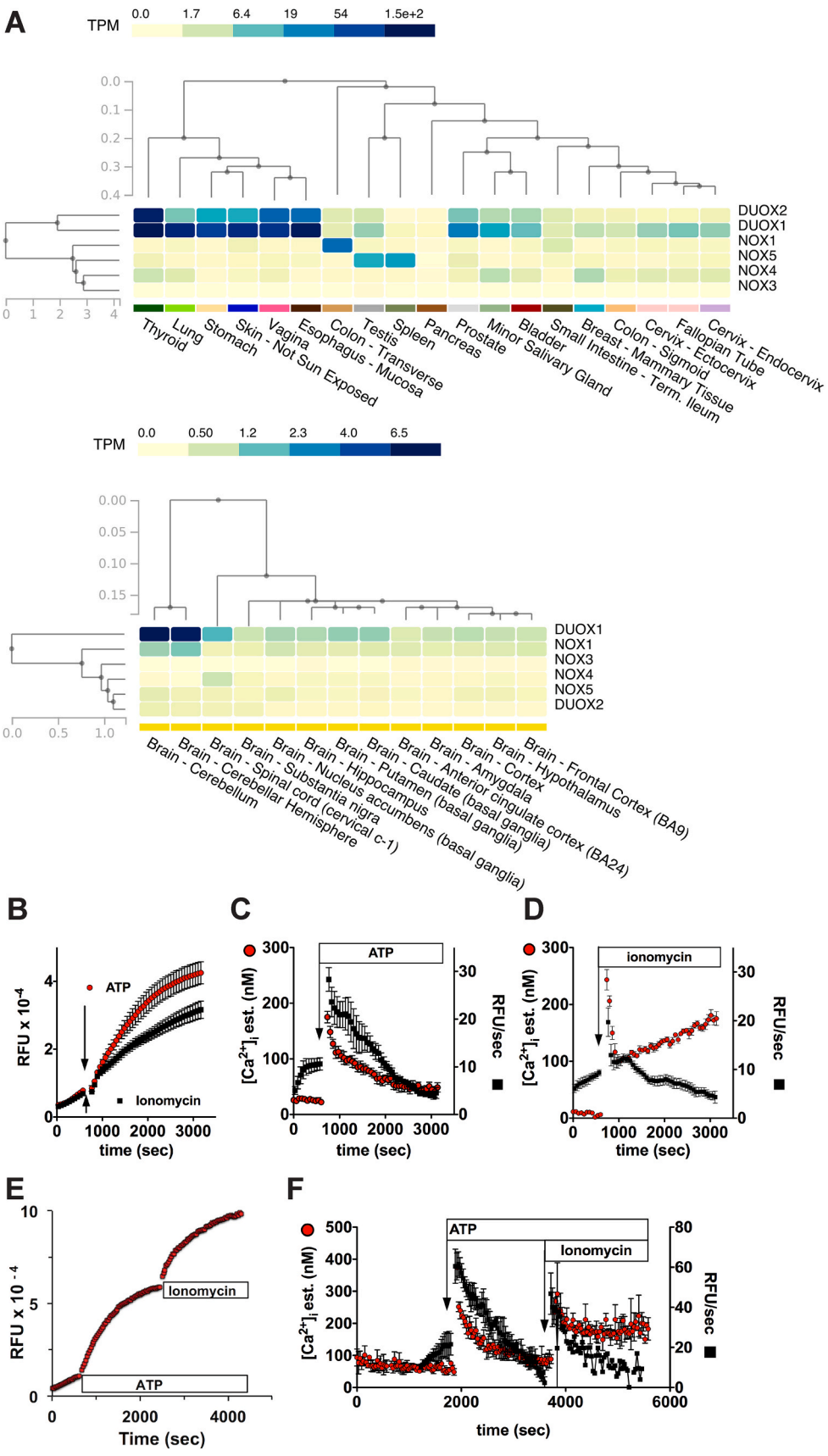

Fig. 1. Duox activity is terminated without renormalization of intracellular calcium. ***Panel A,*** **Heat map of NADPH oxidase mRNA expression in human tissues shows DUOX1 and DUOX2 are the major non-phagocytic NOX forms in most epithelial tissues and DUOX1 is the major form in brain. This highlights the potential importance of Duox in these tissues. The data used for these analyses were obtained from the GTEx Portal on 07/27/2020. The Genotype-Tissue Expression (GTEx) Project was supported by the Common Fund of the Office of the Director of the National Institutes of Health, and by NCI, NHGRI, NHLBI, NIDA, NIMH, and NINDS.** *Panels B-F,* NHBE cultures were loaded with Fura-2 and then simultaneously assessed for H_2O_2 synthesis and $[Ca^{2+}]_i$. *Panel B,* H_2O_2 synthesis progress curve following stimulation with either ATP (100 μM, red circles) or ionomycin/thapsigargin (10 μM/0.1 μM, black squares). *Panels C and D,* re-expression of data in *Panel B* as H_2O_2 synthesis rate (black squares) and $[Ca^{2+}]_i$ (red circles) determined by Fura-2. Baseline Fura-2 fluorescence was recorded for 30 min before addition of HRP/Amplex red. Ionomycin treatment prevented renormalization of $[Ca^{2+}]_i$ but Duox activity returned toward baseline despite elevated $[Ca^{2+}]_i$ (*Panels B-D*, mean ± s.e.m., n = 6, 2 lung donors). *Panel E,* H_2O_2 synthesis progress curve after sequential stimulation with ATP (100 μM) followed by ionomycin/thapsigargin (10 μM/0.1 μM) stimulation to same culture. *Panel F,* replot of synthesis rate (black squares) from *Panel E* and $[Ca^{2+}]_i$ (red circles) (n = 3 cultures, 1 lung donor, H_2O_2 synthesis rate after ionomycin n = 1). The ionomycin-stimulated activity demonstrated that neither NADPH availability nor HRP/Amplex Red depletion could account for the observed termination of Duox activity after ATP stimulation.

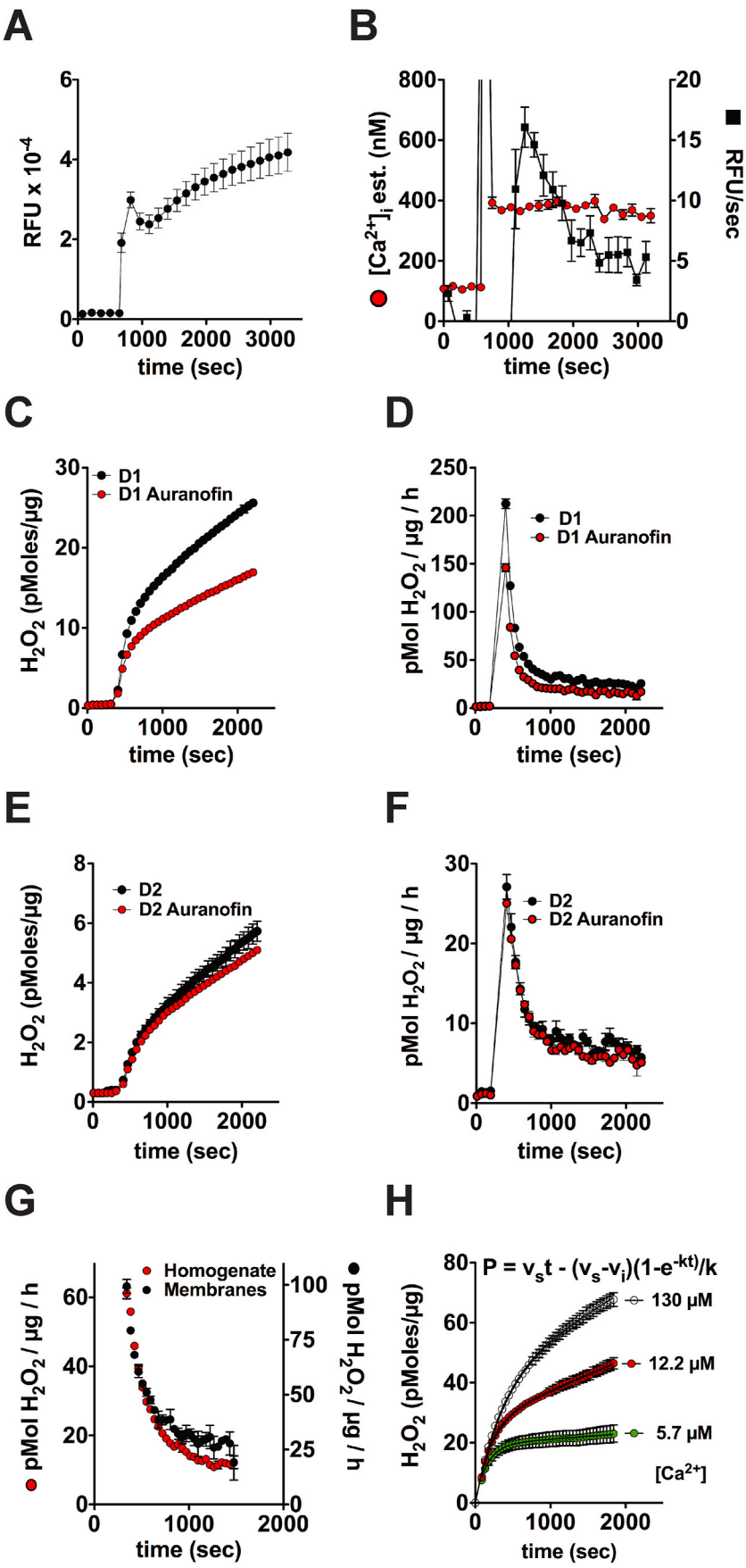

Fig. 2. Duox activity is regulated by a shift to an inactive form. H_2O_2 synthesis was assayed in intact cells, homogenates, and a membrane fraction from HEK293T cells expressing either DUOX1/DUOXA1α or DUOX2/DUOXA2. *Panel A,* H_2O_2 synthesis progress curve following addition of ionomycin/thapsigargin (10 μM/0.1 μM) to intact DUOX1 expressing cells loaded with Fura-2. *Panel B,* replot of panel A data as rate of H_2O_2 synthesis and $[Ca^{2+}]_i$ showing a decrease in H_2O_2 synthesis in elevated $[Ca^{2+}]_i$. *Panels C and D* progress curves and rate plots of DUOX1 cell-free homogenates with and without auranofin (2 μM) using 12 μM Ca^{2+}. *Panel E and F,* progress curves and rate plots of DUOX2 expressing cells±auranofin (2 μM) using 12 μM Ca^{2+}. Auranofin inhibition of GPx and TrxR did not prevent apparent loss of enzyme activity. *Panel G,* rate plots of DUOX2 homogenates and membranes from post-mitochondrial supernatants using 12 μM Ca^{2+}. *Panel H,* progress curves of DUOX2 homogenates assayed in different $[Ca^{2+}]$, fit to the equation shown [20]. 95% confidence levels are plotted and are within the symbols and s.e.m. of the data. All data are means ± s.e.m. n = 3.

account for the activity decrese. The NADPH Km for Duox activity has been variously reported to be 30–100 μM [e.g. 18]. Thus, some activity loss is explained by substrate consumption, but failure to restore activity by NADPH readdition showed that substrate loss alone could not account for the activity decrease. Exact determination of relative contributions of inactivation versus reduced substrate will require purification of each Duox in complex with its accessory protein.

To rule out other explanations for loss of H_2O_2 synthesis, various control experiments were performed (Supplementary Fig. S1). To exclude artifacts arising from real time assays in the presence of Amplex red and HRP, assays were performed in the absence of HRP and Amplex red and H_2O_2 measured after acid addition to stop the reaction and to remove NADPH (Supplementary Figs. S1D and E). The result was recapitulated in these post-hoc H_2O_2 assays. Oxygen consumption was monitored using a fluorescent oxygen sensor and [O_2] was unchanged (Supplementary Fig. S1F). Assays were repeated using the homovanillic acid method (Supplementary Figs. S1G and H), assays were carried out at 37° vs 27°, in phosphate buffer instead of HEPES (Supplementary Fig. S1I), using different Amplex red concentrations (Supplementary Fig. S1J) and with different enzyme concentrations (Supplementary Fig. S1K). In all cases the loss of Duox activity was reproduced. Homogenates were prepared in proteinase inhibitors and these inhibitors were present at active concentrations in reactions (see methods), arguing against proteolytic enzyme inactivation. Preincubation of homogenates in the reaction buffer for 30 min prior to NADPH addition did not reduce H_2O_2 synthesis, ruling out nonspecific denaturation of the enzyme (Supplementary Fig. S1L). Instead, preincubation blunted the termination of activity which most likely cannot be explained by slow Ca^{2+} binding based on Ca^{2+} binding kinetics measured in the homologous NADPH oxidase, NOX5 [19]. Together, these experiments strongly argued against an inconsequential explanation for the observed reduction in synthesis rate.

Inspection of *in vitro* progress curves showed they were similar to burst type progress curves for enzymes that undergo inhibition [20], i.e. that activity was biphasic with an early rapid rate, followed by a variable lower rate. The time course of the early rapid phase was much slower than any expected rate due to pre-steady state kinetics. In homogenates, progress curves in differing [Ca^{2+}] fit with high fidelity to the burst-type product curve [20] (Fig. 2H) that describes a branched pathway with a less active form of enzyme. Thus, Duox regulation is complex, with a short-lived Ca^{2+}-stimulated form and a second less active species that continues catalysis at a much reduced rate in the presence Ca^{2+}, suggesting that Duox shifts between two forms. Changes in [Ca^{2+}] appear to shift the relative contribution of fast and slow rates. This shift from a higher to lower rate generates an epithelial respiratory burst similar to that seen in phagocytic cells and shown in NHBE cells in Fig. 1.

The data strongly support a previously unrecognized idea that DUOX1 and DUOX2 are regulated to limit activity and thus prevent excessive changes in epithelial cytoplasmic redox potential. Duox expressed endogenously in NHBE cells and by heterologous expression in HEK293T cells both exhibited regulation. It seems unlikely that HEK293T cells are identically adapted to high level H_2O_2 synthesis found in NHBE cells suggesting that a different regulatory mechanism may be at work in the heterologous system. Alternatively, HEK293T cells may have altered their transcriptional program in response to high levels of Duox H_2O_2 synthesis to similarly regulate Duox, or that the regulatory mechanism is found in all cells. In addition, it is possible that the regulation is intrinsic to Duox activity, for example, depending directly on synthesized H_2O_2 to modify local redox status.

Since Duox is the major regulatable source of H_2O_2 synthesis in most epithelia and H_2O_2 is key to setting redox potential, this novel mechanism is a potential checkpoint for regulating oxidant dependent reactions. A complete understanding of this mechanism is required to know how redox gradients are setup and restricted during cell signaling and cellular differentiation. Loss of this mechanism for downregulation could result in a variety of damaging changes and could contribute to elevated reactive oxygen species report in a variety of pathological states.

Funding

This work was supported by the Department of Cell Biology Incentive Fund.

Declaration of competing interest

The author declares no competing interests.

Acknowledgments

I thank Monica Valencia Gattas for technical assistance with experiments shown in Fig. 1, panels E and F, and Drs. Joan Burgueno and Nevis Fregien for helpful comments on the manuscript.

Appendix A. Supplementary data

Supplementary data to this article can be found online at https://doi.org/10.1016/j.redox.2021.101931.

References

[1] N. Di Marzo, E. Chisci, R. Giovannoni, The role of hydrogen peroxide in redox-dependent signaling: homeostatic and pathological responses in mammalian cells, Cells 7 (10) (2018).
[2] A. Donko, Z. Peterfi, A. Sum, T. Leto, M. Geiszt, Dual oxidases, Philos. Trans. R. Soc. Lond. B Biol. Sci. 360 (1464) (2005) 2301–2308.
[3] F. Aslund, M. Zheng, J. Beckwith, G. Storz, Regulation of the OxyR transcription factor by hydrogen peroxide and the cellular thiol-disulfide status, Proc. Natl. Acad. Sci. U.S.A. 96 (11) (1999) 6161–6165.
[4] J. Foreman, V. Demidchik, J.H. Bothwell, P. Mylona, H. Miedema, M.A. Torres, P. Linstead, S. Costa, C. Brownlee, J.D. Jones, J.M. Davies, L. Dolan, Reactive oxygen species produced by NADPH oxidase regulate plant cell growth, Nature 422 (6930) (2003) 442–446.
[5] F. Wu, Y. Chi, Z. Jiang, Y. Xu, L. Xie, F. Huang, D. Wan, J. Ni, F. Yuan, X. Wu, Y. Zhang, L. Wang, R. Ye, B. Byeon, W. Wang, S. Zhang, M. Sima, S. Chen, M. Zhu, J. Pei, D.M. Johnson, S. Zhu, X. Cao, C. Pei, Z. Zai, Y. Liu, T. Liu, G.B. Swift, W. Zhang, M. Yu, Z. Hu, J.N. Siedow, X. Chen, Z.M. Pei, Hydrogen peroxide sensor HPCA1 is an LRR receptor kinase in Arabidopsis, Nature 578 (7796) (2020) 577–581.
[6] T.C. Meng, T. Fukada, N.K. Tonks, Reversible oxidation and inactivation of protein tyrosine phosphatases in vivo, Mol. Cell. 9 (2) (2002) 387–399.
[7] R. Sugamata, A. Donko, Y. Murakami, H.E. Boudreau, C.F. Qi, J. Kwon, T.L. Leto, Duox1 regulates primary B cell function under the influence of IL-4 through BCR-mediated generation of hydrogen peroxide, J. Immunol. 202 (2) (2019) 428–440.
[8] J. Kwon, K.E. Shatynski, H. Chen, S. Morand, X. de Deken, F. Miot, T.L. Leto, M. S. Williams, The nonphagocytic NADPH oxidase Duox1 mediates a positive feedback loop during T cell receptor signaling, Sci. Signal. 3 (133) (2010) ra59.
[9] J.D. Lambeth, A.S. Neish, Nox enzymes and new thinking on reactive oxygen: a double-edged sword revisited, Annu. Rev. Pathol. 9 (2014) 119–145.
[10] S. Rigutto, C. Hoste, H. Grasberger, M. Milenkovic, D. Communi, J.E. Dumont, B. Corvilain, F. Miot, X. De Deken, Activation of dual oxidases Duox1 and Duox2: differential regulation mediated by camp-dependent protein kinase and protein kinase C-dependent phosphorylation, J. Biol. Chem. 284 (11) (2009) 6725–6734.
[11] Y. Nakamura, S. Ohtaki, Extracellular ATP-induced production of hydrogen peroxide in porcine thyroid cells, J. Endocrinol. 126 (2) (1990) 283–287.
[12] R. Forteza, M. Salathe, F. Miot, R. Forteza, G.E. Conner, Regulated hydrogen peroxide production by Duox in human airway epithelial cells, Am. J. Respir. Cell Mol. Biol. 32 (5) (2005) 462–469.
[13] N. Fortemaison, F. Miot, J.E. Dumont, S. Dremier, Regulation of H2O2 generation in thyroid cells does not involve Rac1 activation, Eur. J. Endocrinol. 152 (1) (2005) 127–133.
[14] M. Hristova, C. Veith, A. Habibovic, Y.W. Lam, B. Deng, M. Geiszt, Y.M. Janssen-Heininger, A. van der Vliet, Identification of DUOX1-dependent redox signaling through protein S-glutathionylation in airway epithelial cells, Redox biology 2 (2014) 436–446.
[15] H.J. Forman, M. Torres, Reactive oxygen species and cell signaling: respiratory burst in macrophage signaling, Am. J. Respir. Crit. Care Med. 166 (12 Pt 2) (2002) S4–S8.
[16] M.V. Gattas, A. Jaffe, J. Barahona, G.E. Conner, Proton channel blockers inhibit Duox activity independent of Hv1 effects, Redox biology 28 (2020) 101346.
[17] F. Radenkovic, O. Holland, J.J. Vanderlelie, A.V. Perkins, Selective inhibition of endogenous antioxidants with Auranofin causes mitochondrial oxidative stress which can be countered by selenium supplementation, Biochem. Pharmacol. 146 (2017) 42–52.

[18] A.M. Leseney, D. Deme, O. Legue, R. Ohayon, P. Chanson, J.P. Sales, D. Pires de Carvalho, C. Dupuy, A. Virion, Biochemical characterization of a Ca2+/NAD(P)H-dependent H2O2 generator in human thyroid tissue, Biochimie 81 (4) (1999) 373–380.
[19] C.C. Wei, N. Motl, K. Levek, L.Q. Chen, Y.P. Yang, T. Johnson, L. Hamilton, D. J. Stuehr, Conformational States and kinetics of the calcium binding domain of NADPH oxidase 5, Open Biochem. J. 4 (2010) 59–67.
[20] S.G. Waley, The kinetics of substrate-induced inactivation, Biochem. J. 279 (Pt 1) (1991) 87–94.
[21] M.C. Nlend, R.J. Bookman, G.E. Conner, M. Salathe, Regulator of G-protein signaling protein 2 modulates purinergic calcium and ciliary beat frequency responses in airway epithelia, Am. J. Respir. Cell Mol. Biol. 27 (4) (2002) 436–445.
[22] M.L. Fulcher, S. Gabriel, K.A. Burns, J.R. Yankaskas, S.H. Randell, Well-differentiated human airway epithelial cell cultures, Methods Mol. Med. 107 (2005) 183–206.